# CMIP5 Projections of Arctic Amplification, of the North American/North Atlantic Circulation, and of Their Relationship

ELIZABETH A. BARNES

*Department of Atmospheric Science, Colorado State University, Fort Collins, Colorado*

LORENZO M. POLVANI

*Department of Applied Physics and Applied Mathematics, and Department of Earth and Environmental Sciences, and Lamont-Doherty Earth Observatory, Columbia University, New York, New York*

(Manuscript received 21 August 2014, in final form 13 March 2015)

ABSTRACT

Recent studies have hypothesized that Arctic amplification, the enhanced warming of the Arctic region compared to the rest of the globe, will cause changes in midlatitude weather over the twenty-first century. This study exploits the recently completed phase 5 of the Coupled Model Intercomparison Project (CMIP5) and examines 27 state-of-the-art climate models to determine if their projected changes in the midlatitude circulation are consistent with the hypothesized impact of Arctic amplification over North America and the North Atlantic.

Under the largest future greenhouse forcing (RCP8.5), it is found that every model, in every season, exhibits Arctic amplification by 2100. At the same time, the projected circulation responses are either opposite in sign to those hypothesized or too widely spread among the models to discern any robust change. However, in a few seasons and for some of the circulation metrics examined, correlations are found between the model spread in Arctic amplification and the model spread in the projected circulation changes. Therefore, while the CMIP5 models offer some evidence that future Arctic warming may be able to modulate some aspects of the midlatitude circulation response in some seasons, the analysis herein leads to the conclusion that the net circulation response in the future is unlikely to be determined solely—or even primarily—by Arctic warming according to the sequence of events recently hypothesized.

## 1. Introduction

In the last few decades the Arctic has been warming faster than the rest of the globe (e.g., Screen and Simmonds 2010), and the potential for this enhanced warming—known as Arctic amplification (Holland and Bitz 2003)—to impact the atmospheric circulation at other latitudes is as yet unknown. Francis and Vavrus (2012) and Liu et al. (2012) (among others) have suggested that the observed Arctic amplification has already impacted weather in the Northern Hemisphere midlatitudes. The mechanism proposed by these two recent studies can be summarized with the following sequence of events. Enhanced Arctic warming, presumably caused by increasing greenhouse gases and potentially accelerated by sea ice loss, reduces the equator-to-pole temperature gradient at the surface. This causes 1) the midlatitude winds to decelerate, 2) the jet stream to slow down, and 3) the jet to shift equatorward [negative North Atlantic Oscillation (NAO)/Arctic Oscillation response]. Associated with these changes in the midlatitude flow, the large-scale Rossby waves 4) propagate more slowly and 5) amplify in the meridional direction, leading to 6) an increase in the frequency of blocking events, which are known to lead to extreme weather in the Northern Hemisphere midlatitudes (e.g., Black et al. 2004; Dole et al. 2011; Screen and Simmonds 2014). We will refer to this chain of events hereafter as the "FL12 mechanism" [after Francis and Vavrus (2012) and Liu et al. (2012)].

The FL12 mechanism has been very much under debate in the recent literature. Some studies have reported additional observational evidence for the existence of a

*Corresponding author address:* Elizabeth A. Barnes, Department of Atmospheric Science, Colorado State University, 1371 Campus Delivery, Fort Collins, CO 80523.
E-mail: eabarnes@atmos.colostate.edu

DOI: 10.1175/JCLI-D-14-00589.1

link between recent extreme weather and Arctic warming (e.g., Tang et al. 2014; Coumou et al. 2014), while other studies have questioned the validity of the results, as they appear to be highly sensitive to the circulation metrics being analyzed (Screen and Simmonds 2013; Barnes 2013). In addition, several studies have stressed that the observational record is far too short to allow one to detect a clear influence of Arctic warming on weather in the northern midlatitudes with any level of confidence, given the large internal variability inherent in the highly turbulent, eddying flow that is present there (e.g., Screen et al. 2014; Walsh 2014; Barnes et al. 2014). For a more detailed discussion of these recent observational studies we refer readers to Cohen et al. (2014) and Barnes and Screen (2015).

The key idea behind our study, therefore, is to focus on a time period over which the signal-to-noise ratio would be much larger than the one in the short observational record. We accomplish this by exploiting the climate projections recently completed by phase 5 of the Coupled Model Intercomparison Project (CMIP5), and we select the projections with the strongest greenhouse gas forcing [representative concentration pathway 8.5 (RCP8.5)]. These projections show that a very robust Arctic amplification will occur over the twenty-first century. The key question here is whether these same projections also show the circulation changes suggested by the FL12 mechanism.

Recall that climate models have already been extensively used to investigate whether reduced Arctic sea ice and the associated near-surface warming can influence the midlatitude circulation. Typically, this is done with carefully designed model experiments, in which Arctic sea ice is artificially reduced (e.g., Deser et al. 2004; Magnusdottir et al. 2004; Deser et al. 2007; Peings and Magnusdottir 2014). In nearly all cases, changes in the circulation are found, supporting the notion that high-latitude sea ice loss is able to affect weather at lower latitudes.

We wish to stress, however, that the key question here is not whether Arctic warming *can* impact midlatitude weather and its extremes, but whether it actually *will* in the manner proposed by Francis and Vavrus (2012) and Liu et al. (2012). In this paper we clearly distinguish between these two questions, and address each one separately using the CMIP5 model output. While the answer to the first question (*can* it?) is, to some degree, already known to be yes (see Barnes and Screen 2015), the answer to the second (*will* it?) has not, to the best of our knowledge, been reported in the literature.

Note that the answer to the second question—whether Arctic amplification *will* impact midlatitude weather following the FL12 mechanism—is not easy to guess a priori, because increasing greenhouse gas concentrations over the twenty-first century are projected to cause significant changes in the global climate at all latitudes, altitudes, and scales (Stocker et al. 2013). For instance, while the lower-tropospheric temperature gradient is projected to decrease, the upper-tropospheric temperature gradient is projected to increase, and it is unclear which gradient the midlatitude circulation will primarily respond to [see an early discussion by Held (1993)]. In fact, recent studies have analyzed the CMIP5 projections of the atmospheric circulation over the twenty-first century and have found significant relationships between the spread in the Northern Hemisphere circulation response among the models and the spread in both upper-tropospheric and lower-tropospheric temperature gradients (Harvey et al. 2014; Haarsma et al. 2013). Thus, even though carefully designed model experiments support the notion that Arctic warming can drive changes in the midlatitude circulation, it is not evident that these effects will be the dominant drivers of the net response of the midlatitude circulation to increased greenhouse gases.

In light of this, we here first seek to determine whether Arctic warming *will*, in fact, cause changes in the midlatitude circulation consistent with the FL12 mechanism. We define, in section 2, six metrics of the midlatitude circulation; these are designed to follow the chain of events from Francis and Vavrus (2012) and Liu et al. (2012) outlined above and capture changes in both the mean flow and the large-scale Rossby waves. Armed with these metrics, in section 3 we show that Arctic warming *will not*, according to the CMIP5 projections, lead to robust midlatitude circulation changes as hypothesized by Francis and Vavrus (2012) and Liu et al. (2012). Then, in section 4, using the intermodel spread, we address the question of whether Arctic warming *can* modulate the midlatitude circulation response and find that while many of the circulation metrics show no correlation at all, some of them are correlated with Arctic warming in some seasons. As summarized in section 5, we conclude that according to the CMIP5 models, Arctic amplification will not be the dominant driver of the projected twenty-first-century circulation changes following the hypothesized chain of events, although there is evidence that it may act to modulate the response.

## 2. Data and methods

### a. CMIP5 model output

To address the questions outlined above, we here analyze the model integrations performed for CMIP5 (Taylor et al. 2012). The 27 models used in this study,

TABLE 1. Data availability of CMIP5 model output. (Expansions of model name acronyms are available online at http://www.ametsoc.org/PubsAcronymList.)

| | Model name | Monthly $u$ and $T$ | Daily $u$, $v$, and Z500 |
|---|---|---|---|
| 1 | BCC_CSM1.1 | x | x |
| 2 | BNU-ESM | x | x |
| 3 | CanESM2 | x | x |
| 4 | CCSM4 | x | |
| 5 | CMCC-CM | x | x |
| 6 | CNRM-CM5 | x | x |
| 7 | CSIRO Mk3.6.0 | x | |
| 8 | FGOALS-g2 | x | x |
| 9 | FGOALS-s2 | | x |
| 10 | GFDL CM3 | x | x |
| 11 | GFDL-ESM2G | x | |
| 12 | GFDL-ESM2M | x | x |
| 13 | GISS-E2-H | x | |
| 14 | GISS-E2-R | x | |
| 15 | HadGEM2-CC | x | x |
| 16 | HadGEM2-ES | x | |
| 17 | INM-CM4.0 | x | |
| 18 | IPSL-CM5A-LR | x | x |
| 19 | IPSL-CM5A-MR | x | x |
| 20 | IPSL-CM5B-LR | x | |
| 21 | MIROC-ESM | x | |
| 22 | MIROC-ESM-CHEM | x | x |
| 23 | MIROC5 | x | x |
| 24 | MPI-ESM-LR | x | x |
| 25 | MPI-ESM-MR | | x |
| 26 | MRI-CGCM3 | x | x |
| 27 | NorESM1-M | x | x |

and their data availability, are listed in Table 1. The key variables we focus on are the monthly mean zonal wind ($u$) and temperature ($T$), as well as the daily mean 500-hPa geopotential height (Z500). In addition, the daily mean 500-hPa zonal and meridional wind ($v$) are used in the blocking identification algorithm. We note that only 16 of the 27 models have all of the necessary data available for this study, but we have chosen to present results for all models with data available. We have confirmed that our conclusions do not change when these 16 models alone are analyzed (not shown). Finally, we wish to underscore that, in order to give equal weight to all models, only a single integration from each model is used, even though ensembles of integrations are available for several models.

Since the goal of this study is to document how the midlatitude circulation, and the accompanying high-latitude warming, will evolve as a consequence of increased anthropogenic greenhouse gas emissions, we analyze the RCP8.5 projections, for which $CO_2$ concentrations nearly quadruple from preindustrial values, and the top-of-atmosphere radiative forcing reaches 8.5 W m$^{-2}$ by the year 2100 (Meinshausen et al. 2011). The midlatitude circulation is notoriously subject to very large internal variability (see, e.g., Deser et al. 2012), so we choose to maximize the signal-to-noise ratio by considering the CMIP5 projections with the largest greenhouse gas forcing.

For this same reason, much of our analysis will focus on the "long term" changes, defined as the difference between the 25-yr periods 2076–99 and 1980–2004 (for the earlier period, data are taken from the CMIP5 historical simulations). However, we will also present projections for the "near term," specifically the period 2020–44, under the same RCP8.5 scenario. The near-term changes may be especially enlightening, given that September sea ice rapidly declines over the period of 2020–44 and is projected to have largely vanished by the latter part of the twenty-first century (e.g., Overland and Wang 2013).

Last, we note that the CMIP5 models differ in their treatment of the atmospheric fields near topography, with some models omitting data for grid points below the surface and other models interpolating the field to provide data at every latitude/longitude grid point and pressure surface. To keep our analysis as simple as possible, we have taken the fields as provided by each model, ignoring missing values when the grid point is below the surface or using the interpolated values when the data are provided.

### b. *Metrics for the midlatitude circulation*

Because the midlatitude circulation in the Northern Hemisphere is far from zonally symmetric, we focus our analysis on the North America/North Atlantic sector, defined as the area within 30°–70°N, 130°–10°W and depicted by the solid white box in Fig. 1. We confine our study to this region in order to remain consistent with our previous work (e.g., Barnes 2013) and, more importantly, because the North America/North Atlantic sector is the region over which claims have been made of observational evidence showing that Arctic amplification might be influencing the midlatitude circulation (e.g., Francis and Vavrus 2012; Liu et al. 2012). Finally, we note that we have experimented with various meridional boundaries and find that our conclusions do not change (not shown).

Given this well-defined region, one next needs to decide which metrics best describe the midlatitude atmospheric circulation. From the hypothesized sequence of events relating Arctic amplification to the midlatitude circulation, it is evident that one needs to analyze both the zonal mean flow and the waves that propagate on such a flow. Attempting to be exhaustive without being overwhelming, we have opted for six metrics for the midlatitude circulation: three for the mean flow and three for the waves (loosely speaking). These metrics are

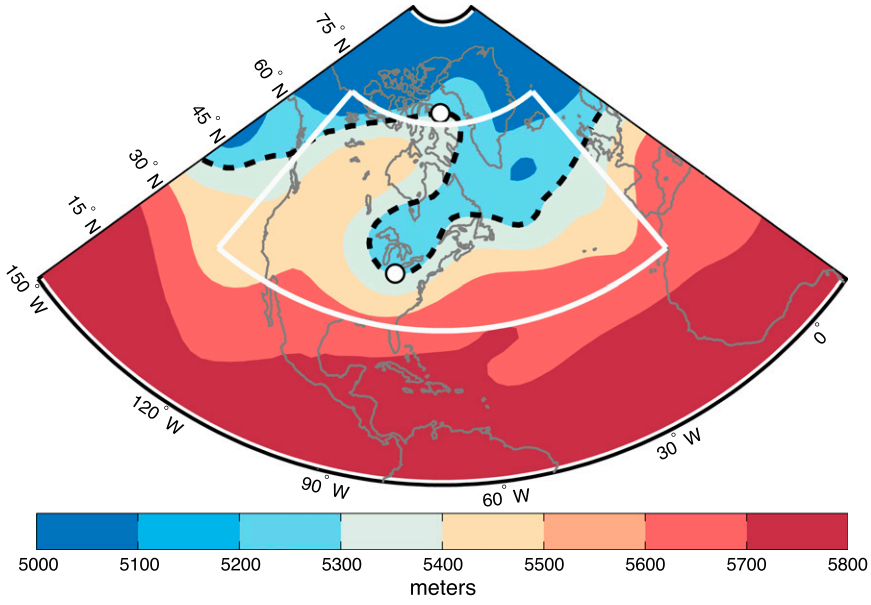


FIG. 1. The North America/North Atlantic sector (white contours) used to define the circulation metrics used in this study. Also shown is the Z500 (shading) on 15 Jan 2005 from the GFDL CM3 historical integration. An example geopotential height isopleth (5350 m) is outlined by the dashed black line, with white circles indicating the day's maximum and minimum latitudes over the North America/North Atlantic region.

meant to roughly capture the stages of the FL12 mechanism, which was summarized in the previous section. Some of the metrics are very easy to compute from model output, while others require more complex computations. For the latter, only a brief sketch of the methods is given here for completeness, and the reader is referred to earlier publications for full details.

#### 1) ZONAL WIND

This is, in many ways, the most basic indicator of the zonal flow. We define the zonal wind as the 500-hPa zonal wind, averaged over the entire North America/North Atlantic sector defined above. This measure gives a very crude indication as to the future acceleration or deceleration of the midlatitude westerly flow, in the middle troposphere, over the region of interest. This metric was used by Francis and Vavrus (2012), among others.

#### 2) JET SPEED

A more sophisticated understanding of the midlatitude winds recognizes the presence of an actual jet stream. We identify this eddy-driven jet stream by zonally averaging the lower-tropospheric zonal wind (925–700 hPa) over the North America/North Atlantic sector, and fitting a parabola around the maximum of the resulting function of latitude: the magnitude of zonal winds at the maximum defines what we will refer to as the jet speed (e.g., Woollings et al. 2010).

#### 3) JET POSITION

The jet position is simply the latitude of the maximum westerly jet stream, determined as above. Note that, as commonly done in the literature, the lower-tropospheric winds are used to identify the jet, rather than the upper-level winds, in order to avoid capturing the subtropical jet, which is strongest at upper levels and decreases toward the surface (e.g., Woollings et al. 2010). An illustration of this can be seen in the black contours of Fig. 2, which show the multimodel mean North America/North Atlantic sector zonal winds; the vertical dashed lines denote the jet position resulting from our definition using the lower-tropospheric winds. In winter (Fig. 2a), the near-surface westerlies of interest here lie a full 20° northward of the upper-level jet maximum (subtropical jet), whereas in summer (Fig. 2b), the upper-level and lower-level maxima are vertically aligned.

#### 4) WAVE SPEED

The phase speeds of the large-scale Rossby waves are diagnosed on the Z500 field. We limit our analysis to resolved waves with zonal wavenumbers between 2 and 6 to highlight the larger waves. The seasonal power spectra of the anomalous fields are calculated following Randel and Held (1991), with anomalies defined as the deviations from the climatological mean plus the first two Fourier harmonics of the daily climatology

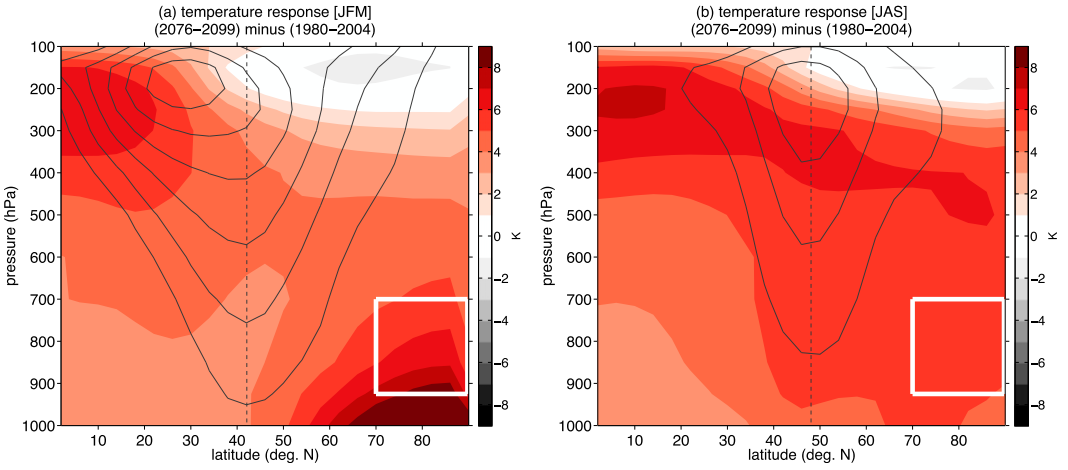


FIG. 2. The multimodel mean air temperature response (shading) between 2076–99 and 1980–2004 under RCP8.5 zonally averaged over the Northern Hemisphere for (a) winter and (b) summer. The white box denotes the region used to calculate the Arctic temperature response and Arctic amplification. Also shown is the North America/North Atlantic jet stream (zonal wind averaged over the sector) contoured every $5\,\mathrm{m\,s^{-1}}$ starting at $5\,\mathrm{m\,s^{-1}}$, with the multimodel mean position of the midlatitude jet stream denoted by the dashed vertical line.

(seasonal cycle). The method used here is identical to the one in Barnes (2013), where all details can be found. The metric that we will refer to as wave speed for the rest of the paper is computed as the mean phase speed of all resolved wavenumbers between 2 and 7 averaged over the North America/North Atlantic sector. We note that we have performed the analysis for wavenumber 2 and wavenumber 5 alone and the conclusions remain qualitatively the same.

#### 5) WAVE EXTENT

We quantify the meridional extent of large-scale propagating Rossby waves using the daily maximum and minimum (DayMaxMin*) metric of Barnes (2013), where again a full description and clear motivation for this metric can be found. In a nutshell, one searches for the maximum and minimum latitude of an individual Z500 isopleth on a single day over a specific longitudinal sector. The dashed black line in Fig. 1 shows an example of such an isopleth (Z500 = 5350 m) on a single day for a single model integration (in this case, the GFDL CM3 historical simulation). The white circles denote the maximum and minimum latitude of the isopleth between the North America/North Atlantic longitudinal boundaries, and DayMaxMin* is defined as the difference between the two. We note that for this calculation, no north/south domain boundary was applied; that is, the North America/North Atlantic domain was relaxed to be 0°–90°N in order to capture the full meridional extent of each wave.

We stress that this metric captures the maximum extent of the wave *on a given day*. We average the daily extents over each season to define the season's average wave extent. One important caveat: following Barnes (2013), we calculate wave extents over an entire range of isopleths (not a single value of Z500), and the change of the wave extents is defined as the difference between the largest extents in the two periods, irrespective of the isopleth. The importance of using a range of isopleths is discussed further in the appendix, where we show why it is misleading to limit the analysis to a single isopleth under global warming conditions. We also show results for only the most extreme wave extents (rather than seasonal averages) in the appendix and discuss changes in wave extent as a function of geographic location (i.e., latitude).

#### 6) BLOCKING

Blocking is diagnosed using the one-dimensional blocking algorithm of Barnes et al. (2012), which identifies blocking regimes as the periods when the Z500 field exhibits a persistent (5 days or longer) reversal of its gradient. Blocked longitudes are grouped in time and space to form a single blocking regime, and the position of a block is defined as the mean longitude of the blocking regime on its onset day. The precise methods and all parameter values used here are identical to those of Barnes et al. (2014), where further details can be found. The resulting "blocking" metric counts the number of blocks occurring between 130° and 10°W and has units of events per season.

### c. *Definition of Arctic amplification*

To capture the lower-tropospheric temperature changes over the polar cap, we define the Arctic

temperature change as the air temperature difference between the two periods, vertically averaged between the 925- and 700-hPa pressure levels, and area averaged from 70° to 90°N (white boxes in Fig. 2). We have verified that limiting the temperature averaging over the North America/North Atlantic longitudinal sector alone, instead of the entire polar cap, produces similar results.

Earlier studies focused on 2-m air temperatures to document Arctic warming (e.g., Holland and Bitz 2003). However, more recent work has noted that such surface warming is often confined to the lowest levels, and may never reach the midtroposphere, where it is able to influence the lower-latitude circulation (e.g., Screen et al. 2012). For this reason, we have opted to average the Arctic temperatures over the lower troposphere instead of simply taking a near-surface value.

The relative warming of the Arctic compared to the rest of the globe, termed ''Arctic amplification,'' is then defined as the Arctic temperature change over the polar cap divided by the global mean temperature change over the same period. Thus, an Arctic amplification greater than 1 implies that the polar cap warms more than the global mean, and a value between 0 and 1 implies that the Arctic warms less than the global mean.

An illustration of this is given in Fig. 2, which shows the CMIP5 multimodel mean temperature change, in winter and summer, between the period 1980–2004 and the end of the twenty-first century. In winter (Fig. 2a), the Arctic lower troposphere warms substantially more than the tropical lower or upper troposphere, indicating a large Arctic amplification. In summer (Fig. 2b), Arctic warming in the lower troposphere is still larger than that in the midlatitude or tropical lower troposphere, although to a lesser degree than in the winter season.

### d. *Model biases*

This work is based entirely on the projections of the CMIP5 models. However, we note that the CMIP5 models, and indeed nearly all current-generation climate models, exhibit well-known systematic biases in simulating some of the circulation metrics discussed here. For example, most models underestimate North Atlantic blocking frequencies during the cool months and overestimate North Atlantic blocking frequencies during the warm months [see Dunn-Sigouin and Son (2013) or Masato et al. (2013) for a detailed discussion of CMIP5 blocking biases]. In addition, these models also tend to place the jet stream equatorward of its observed position (e.g., Barnes and Polvani 2013).

With this said, there is reason to believe that these models are still capable of capturing the relevant large-scale dynamics relevant to our discussion (see, e.g., Fig. A1a). The hypothesis from Francis and Vavrus (2012) and Liu et al. (2012) is based on large-scale temperature gradients and Rossby wave/jet dynamics, all of which should be adequately simulated by the CMIP5 models. In fact, even a simplified dry dynamical core simulates a slower and more equatorward jet stream in response to warming at the polar surface (Butler et al. 2010), a similar response to that seen in more complex models. Thus, while the CMIP5 model biases necessarily reduce our confidence in the model projections, they are the best tools we currently have for predicting the behavior of the large-scale circulation over the twenty-first century.

### e. *Miscellaneous items*

To conclude this methods section, we clarify a couple of items that might be needed for future reproducibility of the results. First, we here define the four seasons in the following manner: winter [January–March (JFM)], spring [April–June (AMJ)], summer [July–September (JAS)], and fall [October–December (OND)], and use the acronym ANN to denote the annual mean, which is the average change of the four seasons. This particular separation of the seasons is chosen to be consistent with previous studies (e.g., Francis and Vavrus 2012; Barnes 2013): our conclusions are in no way dependent on this choice, and results for other combinations of months are also presented below. Second, we calculate all monthly correlations using 3 months of data, that is, the center month and the two adjacent months (e.g., October denotes a correlation using data from September to November). Third, best-fit lines are calculated using linear-least squares regression, and the slopes significantly different from zero are determined using a two-sided $t$ test at 95% confidence (a bootstrap approach results in similar conclusions). Finally, throughout our discussion, we will define a ''robust response'' as one with large model consensus, that is, when at least 90% of the models agree on the sign of the change.

## 3. Projections of Arctic amplification and circulation changes

### a. *Near-term projections (2020–44)*

We start by considering the near-term projections of both Arctic amplification and the atmospheric circulation changes by contrasting the period 2020–44 to the earlier period 1980–2004. While a large signal-to-noise ratio—needed for a clear emergence of the forced response to increasing greenhouse gases from the large internal variability—might not be realized in the near

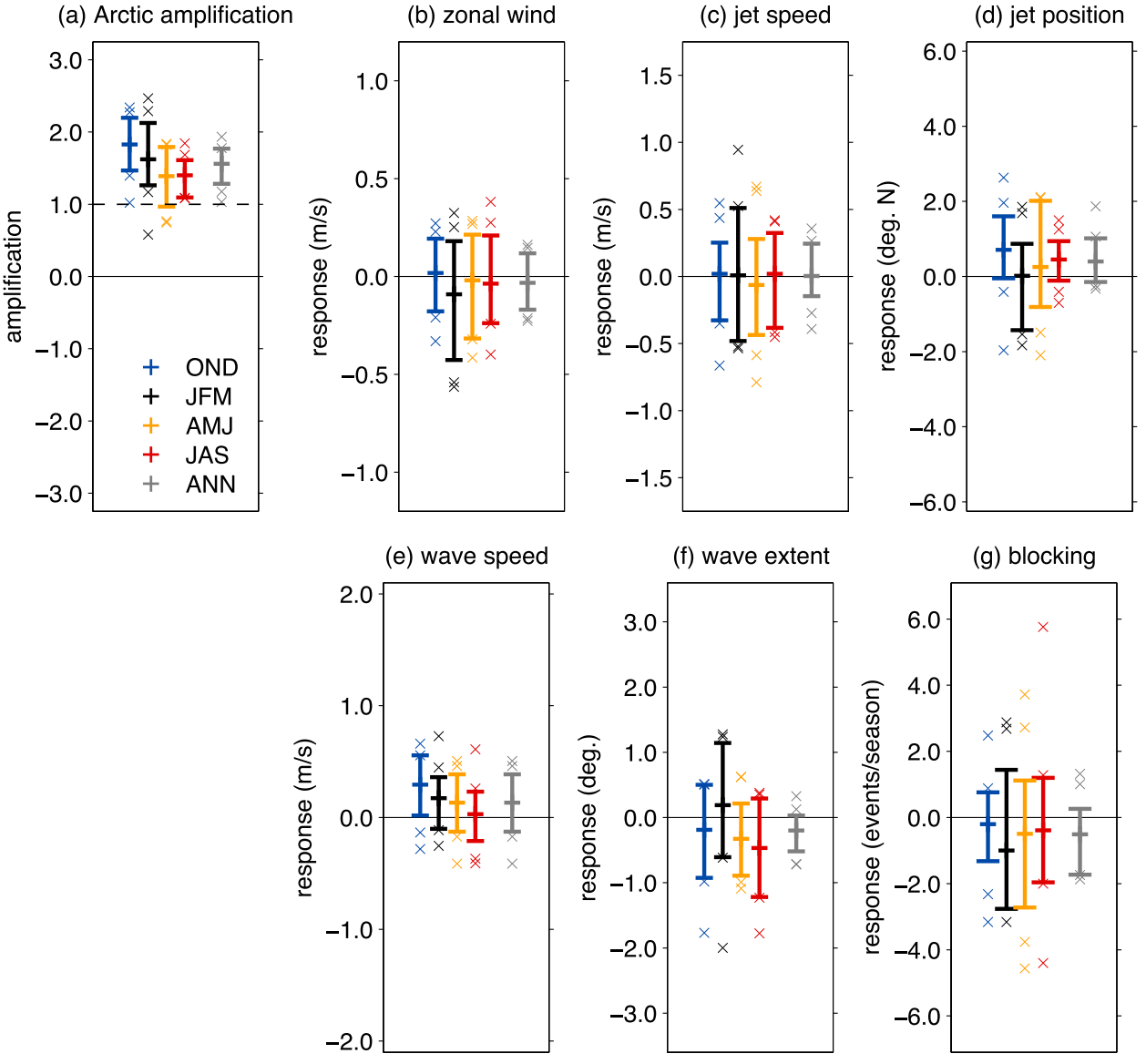


FIG. 3. Seasonal changes in the North America/North Atlantic sector between 2020–44 and 1980–2004 of (a) Arctic amplification, (b) 500-hPa zonal wind change averaged between 30° and 70°N, (c) jet speed, (d) jet shift, (e) 500-hPa geopotential phase speed change for wavenumbers 1–6, (f) maximum DayMaxMin* wave extent, and (g) blocking frequency. Vertical bars denote the 10th–90th percentile range, and crosses denote model responses that fall outside of this range. The horizontal bar denotes the multimodel mean response.

term, these projections are of more immediate concern in terms of climate impacts and adaptation strategies. They are also likely more reliable than the long-term projections at the end of the twenty-first century, as those depend sensitively on the choice of the particular scenario of anthropogenic forcings.

The near-term Arctic amplification, as projected by the CMIP5 models, is shown in Fig. 3a. The different colors correspond to different seasons, with the annual mean value in gray; the vertical bars denote the 10th–90th percentile range, and the crosses indicate models that fall outside of this range. For nearly all seasons and

all models, Arctic amplification is greater than 1, implying that the Arctic will warm more than the rest of the globe in the next few decades. The largest multimodel mean values of Arctic amplification occur in the fall (OND) and winter (JFM), in agreement with the proposed mechanism that Arctic amplification may result from enhanced heat fluxes out of the warmer ocean into the cooler atmosphere during the winter months (e.g., Deser et al. 2010). Note that near-term projections of Arctic amplification are very robust in the annual mean, with all models exhibiting enhanced Arctic warming compared to the global mean.

In stark contrast to this, as one can see from Figs. 3b–g, the CMIP5 models show very little agreement in the near-term projections of the atmospheric circulation, with no metric and/or season combination showing 90% model consensus on the sign of the change. The key point here is that while all CMIP5 models agree that the Arctic will warm 1–2.5 times more than the rest of the globe over the next 30 years, they greatly disagree on the projected changes of the midlatitude circulation.

From this, one can only conclude that Arctic amplification alone (according to the FL12 mechanism) is not an adequate predictor of future changes in the midlatitude circulation. Furthermore, this conclusion applies whether one considers circulation metrics relating to the mean flow, such as zonal wind, jet speed, or jet position (Figs. 3b–d), or metrics relating to the waves, such as wave speed, wave extent, or blocking (Figs. 3e–g). In nearly all cases, the model spread for each metric is large, with little obvious agreement among the models.

### b. *Long-term projections (2076–99)*

Turning now to the long-term projections, we again consider Arctic amplification first. All models in all seasons exhibit Arctic amplification greater than one for the period 2076–99 (Fig. 4a). Note, interestingly enough, that the long-term values of Arctic amplification are quite similar to the near-term values. That is, while the Arctic warms continuously throughout the entire twenty-first century, its relative warming compared to the entire globe appears to change little over time. In contrast, as one can see in Figs. 4b–g, the long-term projected changes in the atmospheric circulation at midlatitudes are different from the near-term changes, with more model agreement in the sign of the response at the end of the twenty-first century.

Let us first focus on the metrics relating to the zonal mean flow. For the first two metrics, zonal wind and jet speed (Figs. 4b,c), the CMIP5 models show *no consensus* on the sign of the projected changes over the North America/North Atlantic domain. For the third, the latitudinal jet position, the CMIP5 models indicate the North American/North Atlantic jet will shift poleward, not equatorward, in all seasons except winter, by the end of the twenty-first century (Fig. 4d). In winter, there is no model agreement in the sign of the change.

Let us next consider the circulation metrics relating to the waves. First, the phase speeds of the large-scale Rossby waves exhibit a robust *increase*, not decrease, in fall, and there is no robust model agreement in the other seasons (Fig. 4e). Chen and Held (2007) argued that recent austral increases in phase speed may be tied to the observed poleward shift of the midlatitude jet. This relationship, however, does not appear to hold for the North American/North Atlantic sector: in summer the jet is projected to shift poleward, but wave speed projections are spread about zero (cf. the red bars in Figs. 4d and 4e). Also, note that every model shows increased wave phase speeds in fall, but there is no model consensus of the sign of the zonal wind response in this season: therefore changes in wave speed cannot be simply described as Doppler shifts induced by an acceleration of the large-scale flow.

Second, the CMIP5 models robustly project *decreases* in wave extents by the end of the twenty-first century, in spring and summer (Fig. 4f). In winter, there is no model consensus on the sign of the change. These findings directly contradict the FL12 mechanism, which suggests that wave extents should increase in the future as a consequence of Arctic amplification. In the appendix, we show that these CMIP5 projections of decreased wave extents are highly robust and do not depend of the details of the method used to compute them.

Third, we find that annual mean blocking frequencies robustly *decrease* (Fig. 4f). Blocking frequency is well known to be dynamically linked to the latitude of the jet stream (e.g., Shabbar et al. 2001; Barriopedro et al. 2006; Croci-Maspoli et al. 2007; Woollings et al. 2008), and Barnes and Hartmann (2010) suggested that models with larger poleward shifts of the jet stream exhibit larger decreases in blocking. This relationship, however, appears to break in winter for the CMIP5 model projections: in many of the models blocking is seen to decrease while the jet shift is broadly spread about zero in that season. This discrepancy could be due to the known model biases in the representation of blocking as already noted in the previous section.

The entire Fig. 4 can now be summarized as follows: all 27 CMIP5 models analyzed here show enhanced Arctic warming by the end of the twenty-first century, yet only a few of the circulation responses are robust. In the instances where there is substantial model agreement, the responses are directly opposite to what is expected from the FL12 mechanism.

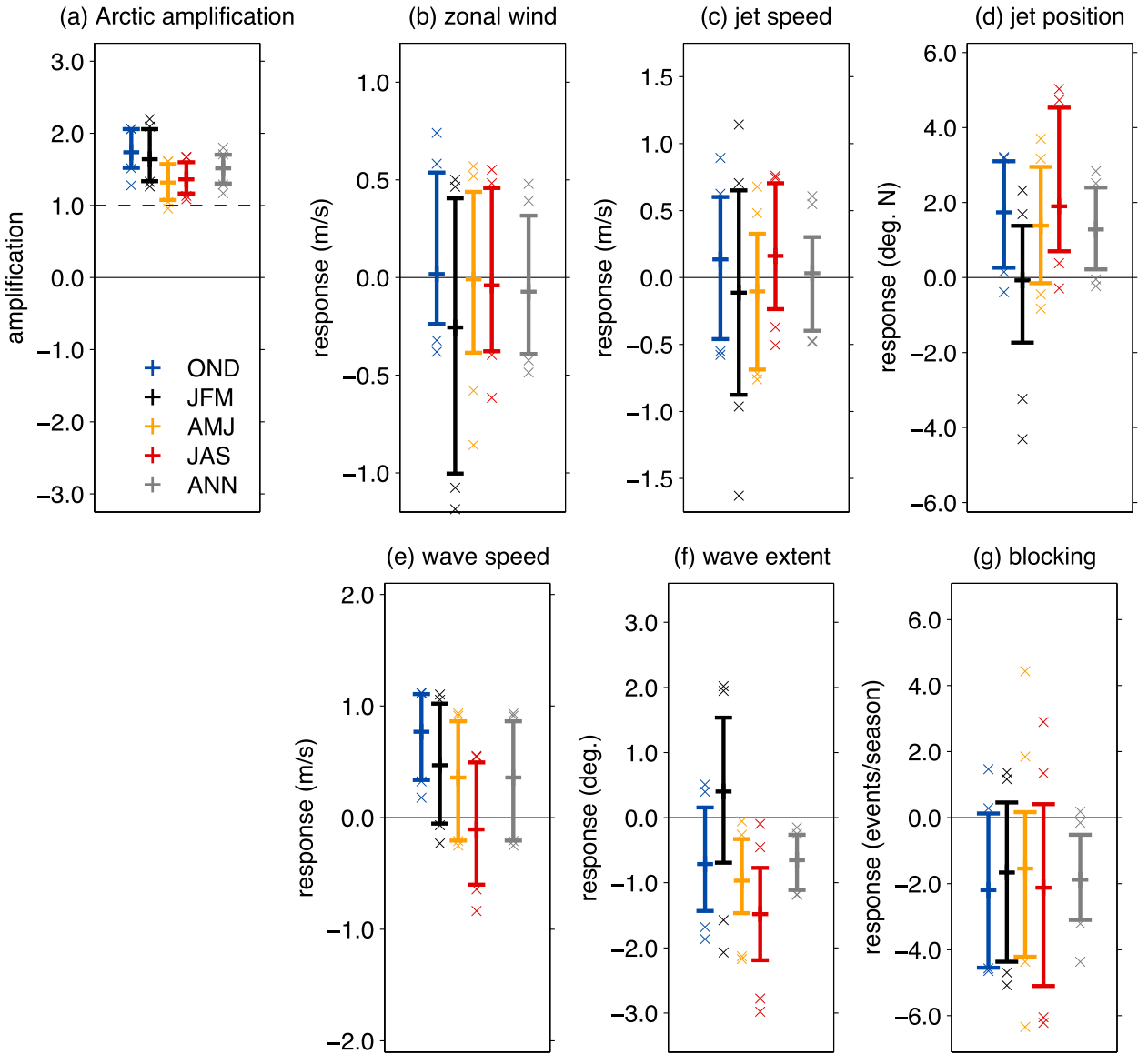


FIG. 4. As in Fig. 3, but for the end of the twenty-first-century changes defined as the difference between 2076–99 and 1980–2004.

## 4. Relationships between Arctic amplification and circulation changes

Although the CMIP5 models suggest that Arctic amplification alone will not be the dominant driver of future changes in the midlatitude circulation over the North America/North Atlantic sector following the FL12 mechanism, it would be simplistic to conclude that Arctic amplification has no role to play at all. In this section we demonstrate that, for some of the circulation metrics we have been considering, the model spread in the long-term circulation changes can be explained, to some degree, by the model spread in Arctic amplification. That is, Arctic amplification may modulate the future circulation response of specific metrics in specific seasons. In this section we focus on the long-term changes alone to bring out the clearest signal.

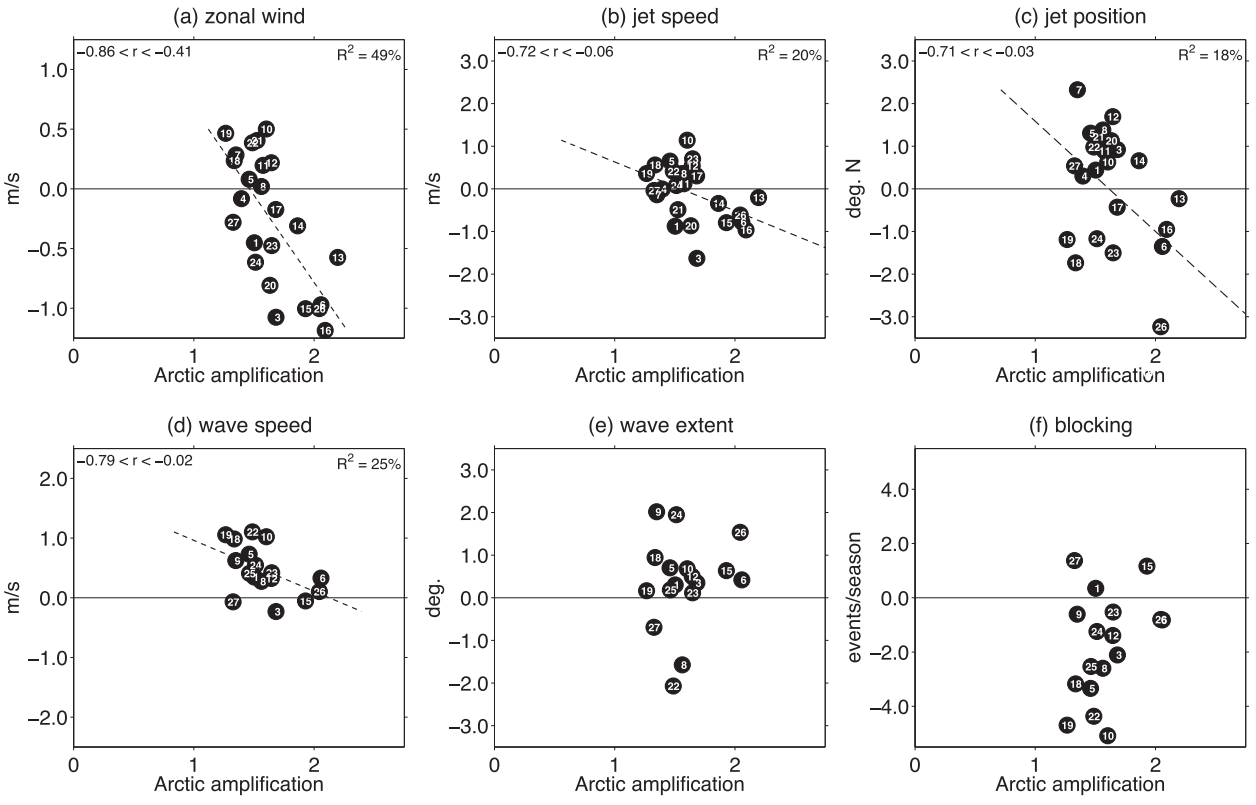


FIG. 5. Long-term changes in the wintertime (JFM) North America/North Atlantic circulation metrics vs Arctic amplification. Responses are defined as changes between 2076–99 and 1980–2004. Dashed lines denote the linear least squares best fit when the best-fit slope is statistically different from zero at 95% confidence. The 95% confidence bounds for the correlation are shown in the top-left corner of each panel and the variance explained in the top-right corner. Each dot denotes a different model, and the white numbers correspond to the models listed in Table 1.

### *a. Winter relationships*

For clarity of presentation, we start by considering scatterplots of the change in each metric versus Arctic amplification—one dot per model—for the winter season (JFM): these are shown in Fig. 5. We focus on JFM first, since this is the season when modeling studies have suggested that Arctic sea ice loss will most strongly influence the midlatitude circulation (e.g., Deser et al. 2010; Screen et al. 2013). Best-fit lines are only shown for panels with slopes statistically different from zero at 95% confidence, and the 95% confidence limits on the correlations ($r$) are given in the top-left corner of each panel. The variances explained by the significant linear fits ($R^2$) are given in the top-right corner of each panel.

Figure 5a shows that the zonal wind change in the models exhibits a strong correlation with Arctic amplification, with 49% of the model spread in the zonal wind change explained by the model spread in Arctic amplification. Furthermore, the sign of the slope implies that models with larger Arctic amplification exhibit less positive zonal wind in the future. One can interpret this correlation as a thermal wind relationship, whereby a decreased meridional temperature gradient is tied to reduced vertical wind shear and thus slower 500-hPa zonal winds if one assumes fixed surface winds. However, while all of the models exhibit a decreased meridional temperature gradient, some show zonal wind increases, suggesting that thermal wind does not capture the full response.

Similar conclusions are reached for the jet speed (Fig. 5b) and jet position (Fig. 5c): models with larger Arctic amplification exhibit less positive (or more negative) changes in these metrics. Note that, for these two variables, the correlations with Arctic amplification are quite weak, with only 20% and 18% of the variance explained, respectively. On the other hand, of the three wave circulation metrics (Figs. 5d–f), only wave speed exhibits significant correlations with Arctic amplification in JFM (although, again, the variance explained is small and the confidence interval for the correlation is large). The negative slope in Fig. 5d implies that larger

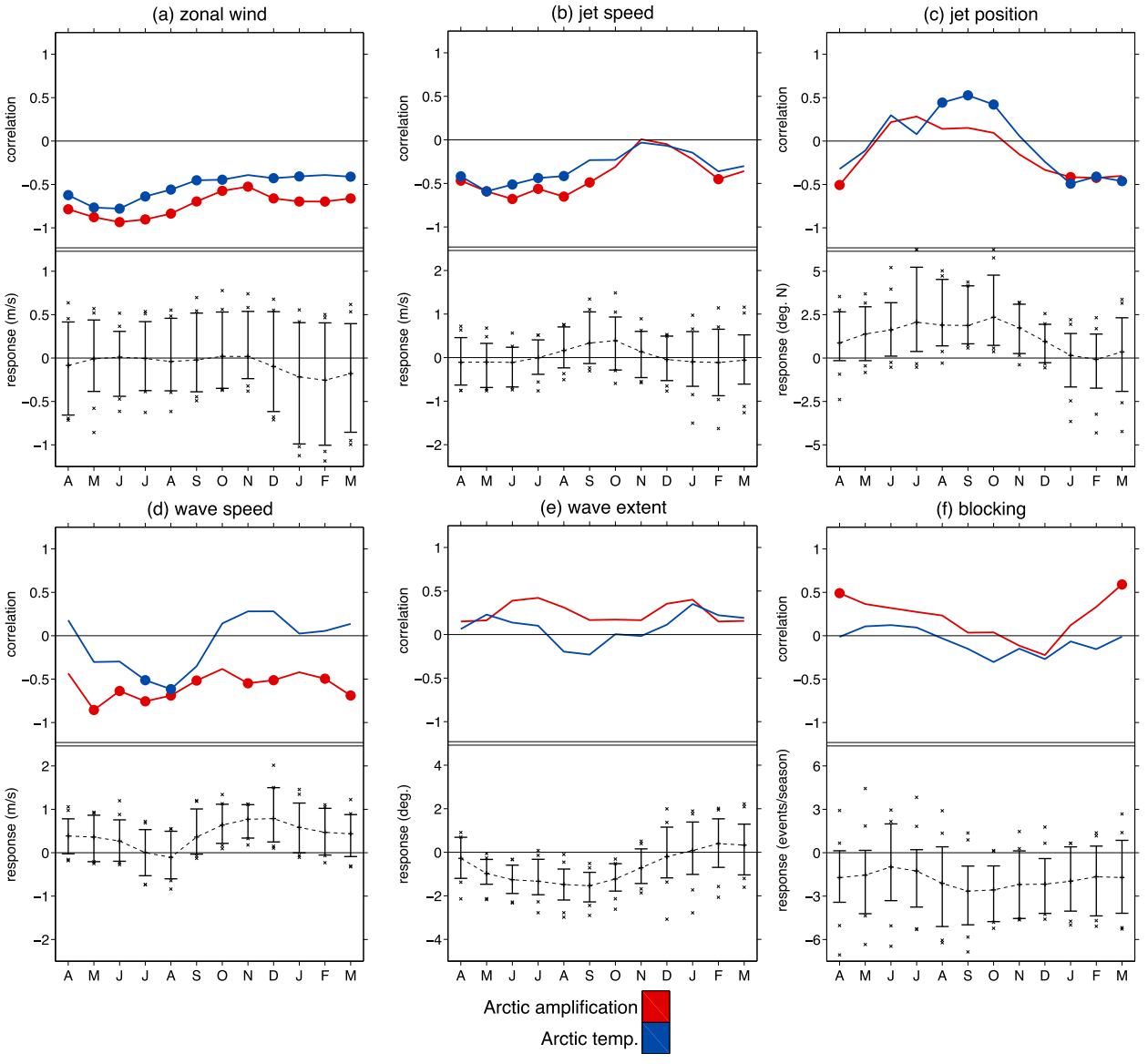


FIG. 6. Correlations of the circulation and temperature responses over the North America/North Atlantic sector for the long-term projections. Colored curves show the correlation as a function of month between the models' Arctic temperature responses and the responses of the respective circulation fields (see text for details). Colored circles denote correlations significant at 95% confidence. Black dashed curves in the bottom half of each panel denote the multimodel mean circulation response as a function of month and bars signify the 10th–90th percentile range with crosses denoting models outside of this range.

Arctic amplification is correlated with *smaller increases* in the phase speeds; as shown in the previous section, most of the models project that waves will accelerate in the long term (see Fig. 4e).

### b. *Monthly relationships*

To broaden our exploration of possible Arctic–midlatitude connections in other seasons, we plot the correlations of all six metrics with Arctic amplification as a function of month in Fig. 6. Since this figure is very rich, we begin with a detailed explanation of Fig. 6a for the zonal wind metric; the other metrics are similarly displayed.

In the upper half of Fig. 6a, the red curve shows the correlation of the zonal wind change, across the models, with the degree of Arctic amplification, across the models. For example, the correlation value for February (−0.7; which includes January and March) comes from the scatterplot already shown in Fig. 5a; the correlations for the other months are calculated similarly. Filled

circles show correlations with statistically significant values. It is clear that the zonal wind change is significantly negatively correlated with Arctic amplification in all months of the year.

The blue curve also displays correlations, but between the absolute change in the Arctic temperatures (without normalization by the global mean temperature change) and the circulation metric. As seen in Fig. 6a, the zonal wind correlations with Arctic amplification (red) and absolute Arctic temperature change (blue) are quite similar, although the correlations with Arctic amplification are more robust and slightly larger throughout the year. Finally, we note that we have performed a similar analysis using the difference between the Arctic and tropical lower-tropospheric temperatures (not shown) and find nearly identical results as those presented here using Arctic amplification (red curve).

In the bottom half of Fig. 6a, the black vertical bars show the zonal wind changes across the models, and are identical to those shown in Fig. 4b, except that they are now plotted as a function of month. The key point here, contrasting the upper and bottom half of Fig. 6a, is that while negative correlations between the zonal wind change and Arctic amplification are significant—so that models with larger Arctic amplification exhibit smaller increases (or larger decreases) in zonal wind by the end of the twenty-first century—the model spread in the zonal wind change is large in all months of the year, and thus the projected net changes are not robust across the models.

Using a similar format, we now examine each of the remaining circulation metrics. Figure 6b shows results for jet speed: unlike zonal wind, the correlations with Arctic amplification here exhibit a marked seasonality, with no significant correlations in fall or winter, the very seasons thought to be most strongly influenced by Arctic amplification. The negative correlations in the spring and summer imply that models with larger Arctic amplification have jet speeds that decrease more (or increase less). However, note again that the change of jet speed is widely spread across zero (bottom half of Fig. 6b). So, while Arctic amplification is negatively correlated with jet speed in the spring/summer, there is no consensus among the models, with half of them showing jet speed increases and the other half showing jet speed decreases during these months.

The jet shift metric shows a yet different behavior. As seen in Fig. 6c, Arctic amplification (red curve) and the Arctic temperature change (blue curve) are negatively correlated with the jet shift in the winter months, with larger Arctic amplification (or Arctic warming) accompanying smaller poleward (or larger equatorward) jet shifts. This is consistent with previous modeling studies that have shown that enhanced Arctic warming drives equatorward jet shifts (negative NAO-like anomalies) (e.g., Magnusdottir et al. 2004; Screen et al. 2013). Thus, it appears that the lack of model agreement in the jet shift in winter (black bars) may be partially explained by the model spread in Arctic warming. Cattiaux and Cassou (2013) have suggested that the weak poleward jet shift in the CMIP5 models in December and January may be linked to Arctic amplification in those months, while the lack of poleward jet shift in February and March may be driven by tropical Pacific teleconnections. Here, we do not find significant correlations between Arctic warming and the jet shift in a November–January average, although we do find significant correlations in averages centered on January through March, when Cattiaux and Cassou (2013) argue Pacific teleconnections may be the driver of the jet shifts.

To add to the complexity, we find that the sign of the correlation is reversed in late summer and early fall (August–October); that is, the absolute change in Arctic temperatures (blue curve) is positively correlated with the jet shift. This offers some evidence that warmer Arctic temperatures might be linked to a more poleward jet in summer. However, additional analysis using the globally averaged temperature change (not shown) suggests that the positive correlations in August–October may actually be a reflection of the models' response to global, rather than local (i.e., Arctic) climate change, as the global temperature change is equally correlated with the jet shift in the warm months.

Wave speeds show significant negative correlations with Arctic amplification throughout most months of the year (Fig. 6d). Again, although the correlations are negative, the net wave speed response tends to positive (i.e., waves are projected to travel faster; bottom half of Fig. 6d). Note also that while phase speed changes are correlated with Arctic amplification, they are not well correlated with the absolute Arctic temperature change.

The final two wave metrics—wave extent (Fig. 6e) and blocking (Fig. 6f)—show weak and largely insignificant correlation with Arctic warming during most of the year. Arctic amplification appears significantly positively correlated with blocking in March and April: however, recall that the monthly correlations are here calculated using data from the two adjacent months, so the March and April correlations share two of the three same months and thus are not independent measures. Once again, the long-term change shows decreased spring and summer blocking by the end of the twenty-first century (bottom half): hence, any positive correlation of blocking frequency with Arctic amplification in early spring does not imply increased blocking frequency in the future.

A final note: one might surmise that the correlations plotted in Fig. 6 are not fundamentally interesting and simply reflect the models' spread in climate sensitivity, that is, that models with large climate sensitivity also produce larger changes in Arctic temperatures, together with changes in midlatitude circulation. To address this possibility, we have performed a similar correlation analysis between the circulation metrics and the global lower-tropospheric temperature. We have found (not shown) that climate sensitivity and Arctic amplification do not show similar correlations, except for the jet position in late summer/early fall (as discussed above). This confirms that the relationships between the circulation and Arctic warming are distinct from the climate sensitivity of the models. A similar disconnect between climate sensitivity and midlatitude circulation changes due to increased $CO_2$ concentrations has been reported in Grise and Polvani (2014).

## 5. Discussion and conclusions

We have examined the climate projections of the CMIP5 models in order to ascertain whether Arctic amplification will impact the atmospheric circulation in the northern midlatitudes in the manner hypothesized by recent studies (Francis and Vavrus 2012; Liu et al. 2012). Our analysis was divided into two main parts. The first quantified the projected responses of six circulation metrics (three mean flow metrics and three wave metrics) between the present day and end of the twenty-first century. We found that every model, in all four seasons, exhibits Arctic amplification by the year 2100, and yet the projected response of the circulation is either in the opposite direction to the one hypothesized, or the spread among the models is too large to discern any robust response.

The second part of the analysis focused on determining whether the spread in the projected responses among the different models could be explained by the corresponding spread in the projected Arctic amplification. We found that the CMIP5 models offer some evidence of this. In particular, enhanced Arctic warming is negatively correlated with the midlatitude mean winds and wave speeds, the jet position exhibits opposite signed correlations depending on the season (positive correlations in summer and negative in winter), and wave extents and blocking events show little to no correlation with Arctic amplification throughout the year.

Many of the correlations found here are consistent with the conclusions of other recent studies. Haarsma et al. (2013) also find that the model spread in the future zonal wind response over the eastern North Atlantic can be largely explained by the model spread in the tropospheric temperature gradient response. In terms of the lack of relationship between Arctic amplification and blocking, Woollings et al. (2014), find no evidence of Arctic warming influencing atmospheric blocking frequency under RCP4.5 or RCP8.5 when the long-term trend is removed from the data. Furthermore, Hassanzadeh et al. (2014) argue that a decrease in the meridional temperature gradient can lead to a decrease (not increase) in midlatitude atmospheric variability (see also Schneider et al. 2015) and blocking frequency.

On the other hand, some of our results appear to be at odds with the conclusions of some recent studies that have focused exclusively on changes of the midlatitude circulation caused by Arctic warming and sea ice loss. In particular, several papers (e.g., Deser et al. 2004, 2007; Butler et al. 2010) have documented that Arctic sea ice loss and/or Arctic warming can induce an equatorward shift of the midlatitude jet. How can we reconcile the results of those studies with the CMIP5 projections discussed here? The answer likely rests in the relative importance of Arctic warming and sea ice loss in comparison to other drivers. As discussed in the introduction, while the lower-tropospheric temperature gradient (the focus here) is projected to decrease in the future, the upper-tropospheric temperature gradient is projected to increase (e.g., Fig. 2). Thus, there is a ''tug of war'' between the warming in the tropics and at the poles (e.g., Held 1993) and it is not immediately obvious who will ultimately ''win.'' In fact, Harvey et al. (2014) show that both the upper- and lower-tropospheric temperature gradients both account for a significant fraction of the CMIP5 model spread in the future storm track response. Deser et al. (2015) demonstrate that Arctic sea ice loss and the associated winter warming of the Arctic surface can account for the absence of a poleward shift of the Northern Hemisphere jet stream in one of the CMIP5 models (CCSM4). Extrapolating these results to the other CMIP5 models, one would expect a negative correlation between the jet shift and Arctic amplification in winter, even if the net jet shift is poleward. This is what we find here. Thus, while the CMIP5 models provide some evidence that Arctic warming *may modulate* certain aspects of the midlatitude circulation response, there is little evidence that Arctic amplification will be sole—or even the dominant—driver of that response in the net.

We conclude by stressing that while the thermodynamic response of the climate to increasing greenhouse gas forcing appears to be largely understood, the dynamic response (i.e., that of the atmospheric circulation) is definitely not (Shepherd 2014). In fact, as shown here,

the models often even disagree on the sign of the response [for a review of this topic, see, e.g., Vallis et al. (2015)]. Thus, there is still much uncertainty not only in the drivers of the circulation response, but also in the response itself. Here, we focused our attention on metrics designed to test the existence of the hypothesized link between Arctic warming and the midlatitude circulation described by Francis and Vavrus (2012) and Liu et al. (2012): however, it is entirely possible that the Arctic may drive midlatitude circulation changes in a manner distinct from the mechanism investigated here. Furthermore, we do not rule out the possibility that the circulation changes will instead drive the Arctic warming in some seasons (e.g., Screen and Simmonds 2013; Graversen et al. 2008; Chung and Räisänen 2011) or that the midlatitude circulation and Arctic temperature changes will be driven by a third (as yet unknown) player.

*Acknowledgments.* We thank three anonymous reviewers for their comments that helped us improve an earlier version of this manuscript. We thank Haibo Liu and the Lamont-Doherty Earth Observatory for obtaining the CMIP5 data and the World Climate Research Programme's Working Group on Coupled Modelling, which is responsible for CMIP. We also thank the climate modeling groups for producing and making available their model output. For CMIP the U.S. Department of Energy's Program for Climate Model Diagnosis and Intercomparison provides coordinating support and led development of software infrastructure in partnership with the Global Organization for Earth System Science Portals. The work of LMP is funded, in part, by a grant from the U.S. National Science Foundation.

## APPENDIX

### Wave Extent Analysis

Here, we provide a more detailed discussion of the response of the meridional wave extents over the North America/North Atlantic region. We calculate the DayMaxMin* meridional wave extent (see methods) for each model over a range of isopleths and Fig. A1a shows the multimodel mean extents for winter (JFM) as a function of isopleth for the historical period (black curve). The model spread is denoted by the dashed lines. The green curve depicts results from the ERA-Interim (Dee et al. 2011), where the wave extents have been calculated identically to those of the CMIP5 models. The isopleths along the *y* axis are oriented such that the isopleths closer to the North Pole are located at the top of each panel.

Both the models and the observations show a peak in wave extent for an isopleth of approximately 5.2 km (denoted by the colored circles in Fig. A1a), and it is this peak wave extent that is used as a diagnostic in Figs. 3f, 4f, 5e, and 6e. The ERA-Interim extents fall well within the spread of the CMIP5 historical extents (dashed lines), highlighting that the models are capable of capturing this measure of observed wave activity.

Figure A1b shows similar curves for the CMIP5 models, but compares the historical (black) with the long-term (red) model projections. Over the twenty-first century, there is a shift in wave activity to larger isopleths; however, one finds that the peak wave extents (colored circles) show very little change (as seen in Fig. 4f). To properly calculate whether the amplitude of the wave extents changes over the twenty-first century, we remove the shift by centering the wave extent curves on the isopleth with the maximum extent, as shown in Fig. A1c. From this, it is clear that the distribution of wave extents about their maximum remains relatively constant with climate warming, with only a small increase (0.4° latitude, or less than a 2% change) in the multimodel mean wave extent for the largest waves (as documented in Fig. 4f). The model spread is very large (dashed curves), with nearly the same number of models showing increases as showing decreases at this location in this season (see Fig. 4f or 6e). This analysis further demonstrates that the results shown in Figs. 3f and 4f are not sensitive to the use of the maximum wave extent as a diagnostic, as all isopleths behave somewhat similarly. Finally, we have repeated the wave extent analysis for all of the four seasons (not shown), and we find either that the results are consistent with what is shown for JFM or that the wave extent distributions exhibit decreases (not increases) over the twenty-first century.

We now address the reason behind this shift of the wave extents to higher isopleths under future climate change. Barnes (2013) argued that a shift in wave activity from one 500-hPa geopotential isopleth to another (as in Fig. A1b) could be due solely to the fact that the high latitudes warm more than low latitudes and thus, by the hypsometric equation, the isopleths shift poleward. In this instance, the wave extents and the latitude of wave activity could remain unchanged but the response to increases in greenhouse gas concentrations would manifest itself as a shift in the wave extents to higher isopleths, as is suggested by the shift in Fig. A1b. To test how much of the model wave extent response in Fig. A1b is due to this simple hypsometric effect, Fig. A1d shows the same curves as in Fig. A1b but with

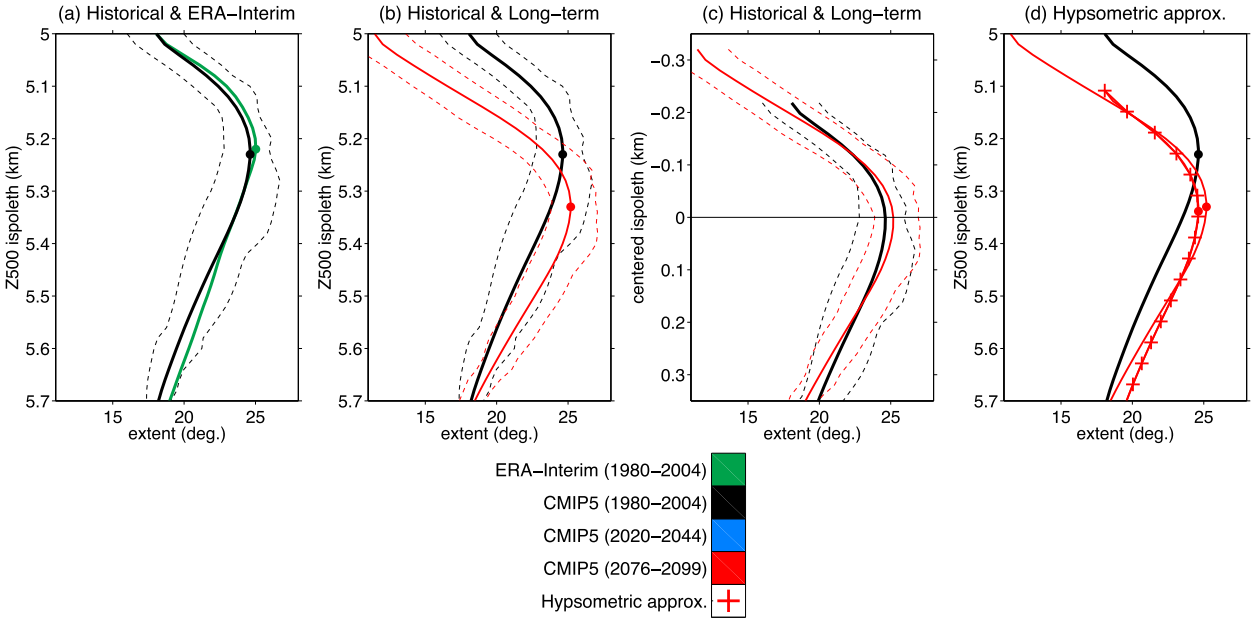


FIG. A1. (a),(b) JFM mean daily wave extent as a function of Z500 isopleth for the historical (1980–2004; black) and long-term (2076–99; red) with the green line in (a) denoting 1980–2004 values from ERA-Interim. (c) As in (b), except the curves are centered on the multimodel mean isopleth with the maximum extent. (d) As in (b), except the red crosses denote the long-term response explained solely by the hypsometric approximation (see text for details). In all panels, the $y$ axis is oriented so that the North Pole is at the top of each panel. Colored circles denote the position of the multimodel mean maximum extent. Dashed lines denote the 10th–90th percentile range of the models. All curves have been smoothed twice with a nonrecursive 1–2–1 filter.

the long-term response approximated solely by the hypsometric equation (red crosses). The change in the isopleths ($\Delta z$) predicted by the hypsometric equation alone is approximated as follows:

$$\Delta z = \frac{R\Delta\overline{T}}{g}\ln\left(\frac{p_1}{p_2}\right), \tag{A1}$$

where $\Delta\overline{T}$ is the change in the average temperature of the 1000–500-hPa layer over the polar North American/North Atlantic sector, $p_1 = 1000\,\text{hPa}$, $p_2 = 500\,\text{hPa}$, $R = 287\,\text{J}\,(\text{kg K})^{-1}$ (the specific gas constant for dry air), and $g = 9.8\,\text{m s}^{-1}$ (the gravitational constant).

From Fig. A1d, it is clear that the hypsometric approximation alone (red crosses) can account for nearly the entire multimodel mean response in wave extent by 2100. That is, the red crosses align with the actual long-term response shown in solid red. This strongly supports the idea that the increase in wave extent for a specific isopleth (e.g., 5.4 km) seen in Fig. A1b is mostly due to a shift of wave activity from one isopleth another, rather than a change in the behavior of the waves.

These considerations demonstrate the importance of analyzing wave activity over a large range of isopleths when comparing present-day and future circulations, as an increase in high-latitude temperatures can induce a shift in wave activity from one isopleth to another with no change in the wave dynamics. In this case, it is possible that this effect may be erroneously interpreted as a

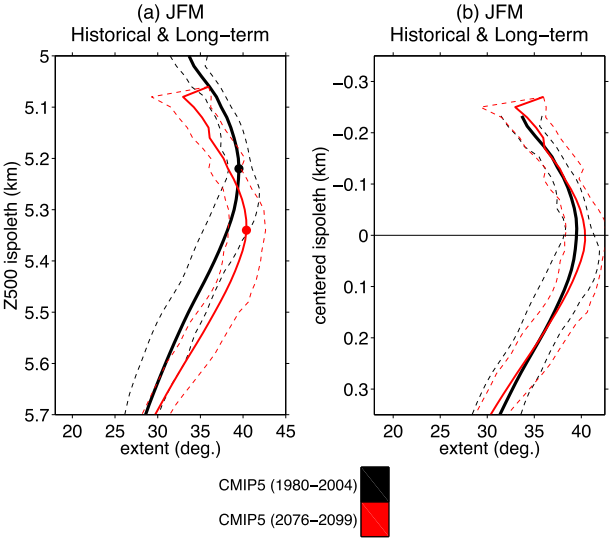


FIG. A2. As in Figs. A1b,c, but for the extreme wave extents defined as the average seasonal 95th percentile wave extent.

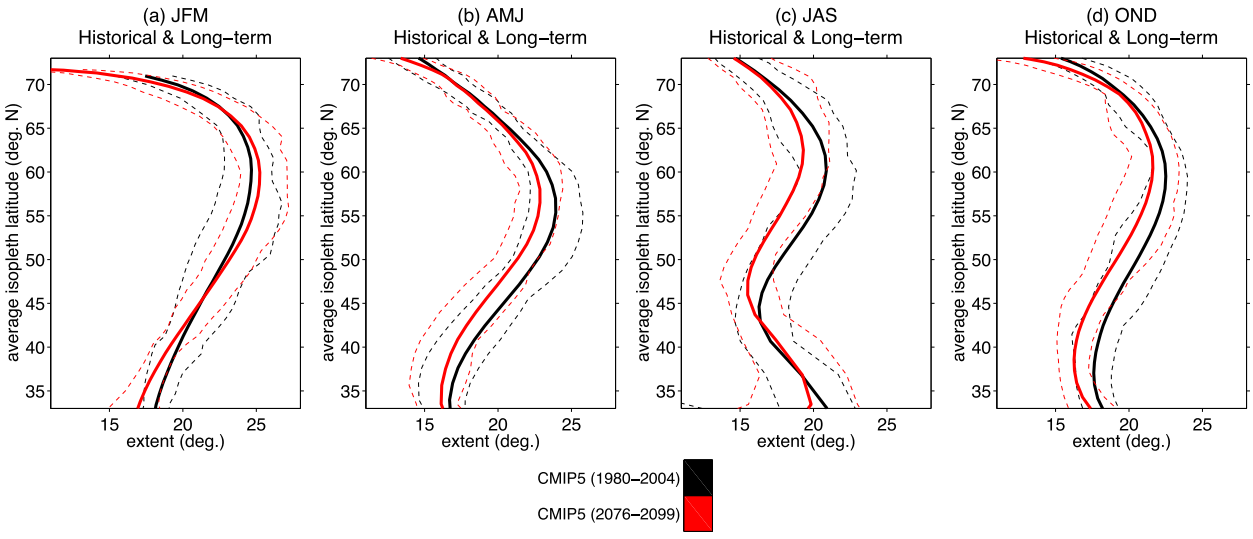


FIG. A3. As in Fig. A1b, but as a function of the average latitude of the isopleth ($y$ axis) and for all four seasons.

change in wave activity if a fixed isopleth is used. When the shift of the geopotential height field with climate warming is accounted for in this analysis, we find that future changes in wave extent are very small and fall well within the historical model spread.

Arctic warming may only influence wave extent extremes; if this is the case, it is possible that our analysis of the mean wave extents may miss these extreme effects. To check whether this is the case, Fig. A2 displays similar panels to those in Figs. A1b and A1c, except for the 95th percentile extent. (The model IPSL-CM5A-LR has been omitted because its high-latitude wave extents in autumn are significant outliers compared to the other 17 CMIP5 models.) The extreme wave extents in Fig. A2a show largely similar behavior to that of the average wave extents (Fig. A1b). From these results, we conclude that analysis of the mean wave extents provides a similar picture to that of the extremes.

Finally, our results provide no indication of how the wave extents over particular geographic locations may respond in the future. Figure A3 displays panels similar to Fig. A1b for all four seasons, except that now the extents are plotted as a function of the average isopleth latitude. The average latitude is determined by calculating the average latitude over the domain of each isopleth each day and then averaging these latitudes together to obtain one representative latitude per isopleth. From this figure, we see that the model spread is large compared to the multimodel mean response in all seasons, and that the conclusions do not depend on whether isopleth or average latitude is used.

## REFERENCES

Barnes, E. A., 2013: Revisiting the evidence linking Arctic amplification to extreme weather in midlatitudes. *Geophys. Res. Lett.,* **40,** 4728–4733, doi:10.1002/grl.50880.

——, and D. L. Hartmann, 2010: Influence of eddy-driven jet latitude on North Atlantic jet persistence and blocking frequency in CMIP3 integrations. *Geophys. Res. Lett.,* **37,** L23802, doi:10.1029/2010GL045700.

——, and L. M. Polvani, 2013: Response of the midlatitude jets, and of their variability, to increased greenhouse gases in the CMIP5 models. *J. Climate,* **26,** 7117–7135, doi:10.1175/JCLI-D-12-00536.1.

——, and J. Screen, 2015: The impact of Arctic warming on the midlatitude jet-stream: Can it? Has it? Will it? *Wiley Interdiscip. Rev.: Climate Change,* **6,** 277–286, doi:10.1002/wcc.337.

——, J. Slingo, and T. Woollings, 2012: A methodology for the comparison of blocking climatologies across indices, models and climate scenarios. *Climate Dyn.,* **38,** 2467–2481, doi:10.1007/s00382-011-1243-6.

——, E. Dunn-Sigouin, G. Masato, and T. Woollings, 2014: Exploring recent trends in Northern Hemisphere blocking. *Geophys. Res. Lett.,* **41,** 638–644, doi:10.1002/2013GL058745.

Barriopedro, D., R. García-Herrera, A. R. Lupo, and E. Hernández, 2006: A climatology of Northern Hemisphere blocking. *J. Climate,* **19,** 1042–1063, doi:10.1175/JCLI3678.1.

Black, E., M. Blackburn, G. Harrison, B. Hoskins, and J. Methven, 2004: Factors contributing to the summer 2003 European heatwave. *Weather,* **59,** 217–223, doi:10.1256/wea.74.04.

Butler, A. H., D. W. J. Thompson, and R. Heikes, 2010: The steady-state atmospheric circulation response to climate change–like thermal forcings in a simple general circulation model. *J. Climate,* **23,** 3474–3496, doi:10.1175/2010JCLI3228.1.

Cattiaux, J., and C. Cassou, 2013: Opposite CMIP3/CMIP5 trends in the wintertime northern annular mode explained by combined local sea ice and remote tropical influences. *Geophys. Res. Lett.,* **40,** 3682–3687, doi:10.1002/grl.50643.

Chen, G., and I. Held, 2007: Phase speed spectra and the recent poleward shift of Southern Hemisphere surface westerlies. *Geophys. Res. Lett.,* **34,** L21805, doi:10.1029/2007GL031200.

Chung, C. E., and P. Räisänen, 2011: Origin of the Arctic warming in climate models. *Geophys. Res. Lett.,* **38,** L21704, doi:10.1029/2011GL049816.

Cohen, J., and Coauthors, 2014: Recent Arctic amplification and extreme mid-latitude weather. *Nat. Geosci.,* **7,** 627–637, doi:10.1038/ngeo2234.

Coumou, D., V. Petoukhov, S. Rahmstorf, S. Petri, and H. Schellnhuber, 2014: Quasi-resonant circulation regimes and hemispheric synchronization of extreme weather in boreal summer. *Proc. Natl. Acad. Sci. USA,* 111, 12 331–12 336, doi:10.1073/pnas.1412797111.

Croci-Maspoli, M., C. Schwierz, and H. C. Davies, 2007: Atmospheric blocking: Space-time links to the NAO and PNA. *Climate Dyn.,* **29,** 713–725, doi:10.1007/s00382-007-0259-4.

Dee, D. P., and Coauthors, 2011: The ERA-Interim reanalysis: Configuration and performance of the data assimilation system. *Quart. J. Roy. Meteor. Soc.,* **137,** 553–597, doi:10.1002/qj.828.

Deser, C., G. Magnusdottir, R. Saravanan, and A. Phillips, 2004: The effects of North Atlantic SST and sea ice anomalies on the winter circulation in CCM3. Part II: Direct and indirect components of the response. *J. Climate,* **17,** 877–889, doi:10.1175/1520-0442(2004)017<0877:TEONAS>2.0.CO;2.

——, R. A. Tomas, and S. Peng, 2007: The transient atmospheric circulation response to North Atlantic SST and sea ice anomalies. *J. Climate,* **20,** 4751–4767, doi:10.1175/JCLI4278.1.

——, ——, M. Alexander, and D. Lawrence, 2010: The seasonal atmospheric response to projected Arctic sea ice loss in the late twenty-first century. *J. Climate,* **23,** 333–351, doi:10.1175/2009JCLI3053.1.

——, A. Phillips, V. Bourdette, and H. Teng, 2012: Uncertainty in climate change projections: The role of internal variability. *Climate Dyn.,* **38,** 527–546, doi:10.1007/s00382-010-0977-x.

——, R. Tomas, and L. Sun, 2015: The role of ocean–atmosphere coupling in the zonal-mean atmospheric response to Arctic sea ice loss. *J. Climate,* **28,** 2168–2186, doi:10.1175/JCLI-D-14-00325.1.

Dole, R., and Coauthors, 2011: Was there a basis for anticipating the 2010 Russian heat wave? *Geophys. Res. Lett.,* **38,** L06702, doi:10.1029/2010GL046582.

Dunn-Sigouin, E., and S.-W. Son, 2013: Northern Hemisphere blocking frequency and duration in the CMIP5 models. *J. Geophys. Res. Atmos.,* **118,** 2169–8996, doi:10.1002/jgrd.50143.

Francis, J. A., and S. J. Vavrus, 2012: Evidence linking Arctic amplification to extreme weather in mid-latitudes. *Geophys. Res. Lett.,* **39,** L06801, doi:10.1029/2012GL051000.

Graversen, R., T. Mauritsen, M. Tjernstrom, E. Källén, and G. Svensson, 2008: Vertical structure of recent arctic warming. *Nature,* **451,** 53–56, doi:10.1038/nature06502.

Grise, K. M., and L. M. Polvani, 2014: Is climate sensitivity related to dynamical sensitivity? A Southern Hemisphere perspective. *Geophys. Res. Lett.,* **41,** 534–540, doi:10.1002/2013GL058466.

Haarsma, R. J., W. Hazeleger, C. Severijns, H. de Vries, A. Sterl, R. Bintanja, G. J. van Oldenborgh, and H. W. van den Brink, 2013: More hurricanes to hit Western Europe due to global warming. *Geophys. Res. Lett.,* **40,** 1783–1788, doi:10.1002/grl.50360.

Harvey, B. J., L. C. Shaffrey, and T. J. Woollings, 2014: Equator-to-pole temperature differences and the extra-tropical storm track responses of the CMIP5 climate models. *Climate Dyn.,* **43,** 1171–1182, doi:10.1007/s00382-013-1883-9.

Hassanzadeh, P., Z. Kuang, and B. F. Farrell, 2014: Responses of mid-latitude blocks and wave amplitude to changes in the meridional temperature gradient in an idealized dry GCM. *Geophys. Res. Lett.,* **41,** 5223–5232, doi:10.1002/2014GL060764.

Held, I. M., 1993: Large-scale dynamics and global warming. *Bull. Amer. Meteor. Soc.,* **74,** 228–241, doi:10.1175/1520-0477(1993)074<0228:LSDAGW>2.0.CO;2.

Holland, M. M., and C. M. Bitz, 2003: Polar amplification of climate change in coupled models. *Climate Dyn.,* **21,** 221–232, doi:10.1007/s00382-003-0332-6.

Liu, J., J. Curry, and H. Wang, 2012: Impact of declining Arctic sea ice on winter snowfall. *Proc. Natl. Acad. Sci. USA,* **109,** 4074–4079, doi:10.1073/pnas.1114910109.

Magnusdottir, G., C. Deser, and R. Saravanan, 2004: The effects of North Atlantic SST and sea ice anomalies on the winter circulation in CCM3. Part I: Main features and storm track characteristics of the response. *J. Climate,* **17,** 857–876, doi:10.1175/1520-0442(2004)017<0857:TEONAS>2.0.CO;2.

Masato, G., B. J. Hoskins, and T. J. Woolings, 2013: Winter and summer Northern Hemisphere blocking in CMIP5 models. *J. Climate,* **26,** 7044–7059, doi:10.1175/JCLI-D-12-00466.1.

Meinshausen, M., and Coauthors, 2011: The RCP greenhouse gas concentrations and their extensions from 1765 to 2300. *Climatic Change,* **109,** 213–241, doi:10.1007/s10584-011-0156-z.

Overland, J. E., and M. Wang, 2013: When will the summer Arctic be nearly sea ice free? *Geophys. Res. Lett.,* **40,** 2097–2101, doi:10.1002/grl.50316.

Peings, Y., and G. Magnusdottir, 2014: Response of the wintertime Northern Hemisphere atmospheric circulation to current and projected Arctic sea ice decline: A numerical study with CAM5. *J. Climate,* **27,** 244–264, doi:10.1175/JCLI-D-13-00272.1.

Randel, W., and I. Held, 1991: Phase speed spectra of transient eddy fluxes and critical layer absorption. *J. Atmos. Sci.,* **48,** 688–697, doi:10.1175/1520-0469(1991)048<0688:PSSOTE>2.0.CO;2.

Schneider, T., T. Bischoff, and H. Plotka, 2015: Physics of changes in synoptic midlatitude temperature variability. *J. Climate,* **28,** 2312–2331, doi:10.1175/JCLI-D-14-00632.1.

Screen, J. A., and I. Simmonds, 2010: The central role of diminishing sea ice in recent Arctic temperature amplification. *Nature,* **464,** 1334–1337, doi:10.1038/nature09051.

——, and ——, 2013: Exploring links between Arctic amplification and mid-latitude weather. *Geophys. Res. Lett.,* **40,** 959–964, doi:10.1002/grl.50174.

——, and ——, 2014: Amplified mid-latitude planetary waves favour particular regional weather extremes. *Nat. Climate Change,* **4,** 704–709, doi:10.1038/nclimate2271.

——, C. Deser, and I. Simmonds, 2012: Local and remote controls on observed Arctic warming. *Geophys. Res. Lett.,* **39,** L10709, doi:10.1029/2012GL051598.

——, I. Simmonds, C. Deser, and R. Tomas, 2013: The atmospheric response to three decades of observed Arctic sea ice loss. *J. Climate,* **26,** 1230–1248, doi:10.1175/JCLI-D-12-00063.1.

——, C. Deser, I. Simmonds, and R. Tomas, 2014: Atmospheric impacts of Arctic sea-ice loss, 1979–2009: Separating forced change from atmospheric internal variability. *Climate Dyn.,* **43,** 333–344, doi:10.1007/s00382-013-1830-9.

Shabbar, A., J. Huang, and K. Higuchi, 2001: The relationship between the wintertime North Atlantic Oscillation and blocking episodes in the North Atlantic. *Int. J. Climatol.,* **21,** 355–369, doi:10.1002/joc.612.

Shepherd, T. G., 2014: Atmospheric circulation as a source of uncertainty in climate change projections. *Nat. Geosci.,* **7,** 703–708, doi:10.1038/ngeo2253.

Stocker, T., and Coauthors, Eds., 2013: *Climate Change 2013: The Physical Science Basis.* Cambridge University Press, 1535 pp.

Tang, Q., X. Zhang, and J. A. Francis, 2014: Extreme summer weather in northern mid-latitudes linked to a vanishing cryosphere. *Nat. Climate Change,* **4,** 45–50, doi:10.1038/nclimate2065.

Taylor, K. E., R. J. Stouffer, and G. A. Meehl, 2012: An overview of CMIP5 and the experiment design. *Bull. Amer. Meteor. Soc.,* **93,** 485–498, doi:10.1175/BAMS-D-11-00094.1.

Vallis, G., P. Zurita-Gotor, C. Cairns, and J. Kidston, 2015: Response of the large-scale structure of the atmosphere to global warming. *Quart. J. Roy. Meteor. Soc.,* doi:10.1002/qj.2456, in press.

Walsh, J. E., 2014: Intensified warming of the Arctic: Causes and impacts on middle latitudes. *Global Planet. Change,* **117,** 52–63, doi:10.1016/j.gloplacha.2014.03.003.

Woollings, T., B. Hoskins, M. Blackburn, and P. Berrisford, 2008: A new Rossby wave-breaking interpretation of the North Atlantic Oscillation. *J. Atmos. Sci.,* **65,** 609–626, doi:10.1175/2007JAS2347.1.

——, A. Hannachi, and B. Hoskins, 2010: Variability of the North Atlantic eddy-driven jet stream. *Quart. J. Roy. Meteor. Soc.,* **136,** 856–868, doi:10.1002/qj.625.

——, B. Harvey, and G. Masato, 2014: Arctic warming, atmospheric blocking and cold European winters in CMIP5 models. *Environ. Res. Lett.,* **9,** 014002, doi:10.1088/1748-9326/9/1/014002.